

1

**2 Contamination as a major factor in poor Illumina assembly of microbial  
3 isolate genomes**

4

5 Haeyoung Jeong<sup>1,2\*</sup>, Jae-Goo Pan<sup>1</sup> and Seung-Hwan Park<sup>1,2</sup>

6

7

<sup>8</sup> <sup>1</sup>Infectious Disease Research Center, Korea Research Institute of Bioscience and Biotechnology

(KRIBB), 125 Gwahak-ro, Yuseong-gu, Daejeon 34141, Republic of Korea

10 <sup>2</sup> Biosystems and Bioengineering Program, University of Science and Technology (UST), 217

11 Gajeong-ro, Yuseong-gu, Daejeon 34113, Republic of Korea

12

13

14 \*Corresponding author: [hyeong@kribb.re.kr](mailto:hyeong@kribb.re.kr)

15

16 Running title: Contamination affects microbial genome assemblies

17

18

## ABSTRACT

19

20 The nonhybrid hierarchical assembly of PacBio long reads is becoming the most preferred method  
21 for obtaining genomes for microbial isolates. On the other hand, among massive numbers of  
22 Illumina sequencing reads produced, there is a slim chance of re-evaluating failed microbial  
23 genome assembly (high contig number, large total contig size, and/or the presence of low-depth  
24 contigs). We generated Illumina-type test datasets with various levels of sequencing error,  
25 pretreatment (trimming and error correction), repetitive sequences, contamination, and ploidy from  
26 both simulated and real sequencing data and applied k-mer abundance analysis to quickly detect  
27 possible diagnostic signatures of poor assemblies. Contamination was the only factor leading to  
28 poor assemblies for the test dataset derived from haploid microbial genomes, resulting in an  
29 extraordinary peak within low-frequency k-mer range. When thirteen Illumina sequencing reads of  
30 microbes belonging to genera *Bacillus* or *Paenibacillus* from a single multiplexed run were  
31 subjected to a k-mer abundance analysis, all three samples leading to poor assemblies showed  
32 peculiar patterns of contamination. Read depth distribution along the contig length indicated that  
33 all problematic assemblies suffered from too many contigs with low average read coverage, where  
34 1% to 15% of total reads were mapped to low-coverage contigs. We found that subsampling or  
35 filtering out reads having rare k-mers could efficiently remove low-level contaminants and greatly  
36 improve the *de novo* assemblies. An analysis of 16S rRNA genes recruited from reads or contigs  
37 and the application of read classification tools originally designed for metagenome analyses can  
38 help identify the source of a contamination. The unexpected presence of proteobacterial reads  
39 across multiple samples, which had no relevance to our lab environment, implies that such  
40 prevalent contamination might have occurred after the DNA preparation step, probably at the place  
41 where sequencing service was provided.

42

43

## INTRODUCTION

44

45 During the last two decades, everyone witnessed how innovations in genome sequencing  
46 technologies have revolutionized almost all fields of biomedical research and application.  
47 Microbiology is one of the main beneficiaries among them, as next-generation genome sequencing  
48 has become the most cost-effective solution to answer questions of function, evolution, and  
49 interaction involving microbes and their surrounding environments (1). In the early years, massive  
50 amounts of low-quality short reads with data types totally different from what we have known have  
51 posed challenges to bioinformatics, especially for *de novo* assembly of genomes using Illumina  
52 sequencing platform (2-4). Recent development and improvement in genome sequencing have  
53 resulted in the availability of several dozen software. We have to choose the most suitable one for a  
54 specific purpose. For example, there are more than forty *de novo* assemblers  
55 ([https://en.wikipedia.org/wiki/Sequence\\_assembly](https://en.wikipedia.org/wiki/Sequence_assembly)). Best practice based on assembler evaluations  
56 (5, 6) or the use of automated assembly workbenches depending on validation or integration of  
57 outputs from multiple assemblers (7, 8) could help us obtain optimal Illumina assemblies of  
58 microbial isolate genomes.

59

The introduction of so-called “third generation sequencing” technologies (9) virtually  
60 monopolized by PacBio’s long-read SMRT™ sequencing data and nonhybrid hierarchical genome  
61 assembly process (HGAP) (10) have greatly facilitated the completion of bacterial genomes using  
62 as few as one SMRT™ cell which usually covers ~100x sequencing depth (11). This approach can  
63 dramatically reduce the labor and cost required for finishing genomes compared to first or second  
64 generation sequencing platforms. There are increasing cases of finishing bacterial genomes of  
65 interest using PacBio platform even in the presence of sequence reads that were produced using  
66 second generation sequencing technologies. However, the previous sequencing reads are not be  
67 usually utilized by HGAP anymore. This implies that more and more draft genome sequences,  
68 whether accurate or inaccurate, will have little chances of being re-evaluated if they are not going  
69 to be completed.

70 Carrying out hundreds of microbial sequencing project using Illumina platform as a usual  
71 customer of sequencing facilities, we encountered cases where *de novo* assembly resulted in too  
72 many contigs. Sometimes these assemblies comprised of short ones with low average coverages.  
73 Sometimes the total contig length was significantly larger than the estimated genome size despite  
74 sufficient sequencing depth. We learned from our experiences that pretreatment of reads, parameter  
75 scanning during the assembly procedure (mostly by changing k-mer length), subsampling reads,  
76 and using assemblers such as Velvet (12) that apply automatic coverage cutoff could improve our  
77 results for some problematic datasets. However, we did not take systematic approaches to find out  
78 the factors causing bad assemblies. Although there are many issues relevant to the inherent  
79 accuracy of large genome assemblies such as missing sequences, order/orientation errors, and  
80 erroneous reconstruction of repeats (13), these are beyond the scope of this study.

81 K-mer frequency analysis is an alignment-free method that is widely used in many aspects of  
82 genome researches, such as estimating genome sizes (14), diagnosing sequencing data quality and  
83 complexity (15), and pretreating massive sequencing reads (16). Theoretically, k-mer abundance in  
84 high-depth sequencing reads from an ideal haploid genome is distributed as a Gaussian with an  
85 average abundance equal to the sequencing depth. Low frequency k-mers represent Illumina-  
86 specific errors, genome heterogeneity, and contamination.

87 In this study, using test datasets and real Illumina sequence reads produced from a single run of  
88 11 *Bacillus* and two *Paenibacillus* strains, we found extraordinary peak of rare k-mers from  
89 samples with failed assemblies due to contamination. We also demonstrated that contamination was  
90 the sole cause that spoiled genome assemblies in this case. Using tools were originally designed for  
91 metagenomics sequence analysis, the proportion of contamination in sequencing data and their  
92 possible source could be inferred. We were able to significantly improve the *de novo* assemblies of  
93 problematic samples by filtering out low abundant k-mers which efficiently eliminated low-level  
94 contamination from the reads.

95

96

97

## MATERIALS AND METHODS

98

### 99 **Construction of test datasets**

100 Illumina reads that were produced from previous studies (17-19), which are available at NCBI  
101 sequence read archive (SRA) under the accessions SRP058110 (*Escherichia coli* BL21),  
102 SRP058116 (*Bacillus subtilis* KCTC 1028), and SRP058417 (*Shigella boydii* ATCC 9210), were  
103 utilized to generate test dataset. 100-fold artificial Illumina reads were also simulated from the  
104 complete genome sequences of *E. coli* BL21 (CP010816.1), *Escherichia coli* K-12 MG1655  
105 (NC\_000913.3), *Saccharomyces cerevisiae* S288c (BK006934.2-BK006949.2, and AJ011856.1),  
106 and diploid yeast *Candida albicans* SC5314 (assembly 22, downloaded from  
107 <http://www.candidagenome.org/>) using ART (20) version 03-19-2015 with parameters -l 101 -ss  
108 HS25 -f 100 -m 400 -s 80. To simulate low-quality sequencing reads, error rate parameters of ART  
109 (-ir 0.00009 -ir2 0.00015 -dr 0.00011 -dr2 0.00023 for default setting) were multiplied  
110 appropriately. Unless otherwise mentioned, real Illumina reads were cut at 100x sequencing depth  
111 before being further processed.

### 112 **Bacterial strains, growth condition, and genome sequencing**

113 Eleven *Bacillus* and two *Paenibacillus* strains chosen for genome sequencing are listed in Table 1.  
114 They are probiotic strains isolated from Korean traditional food (21), endophytic bacteria from  
115 cactus, and strains deliberately chosen from culture collection for biotechnological applications.  
116 Cells were grown aerobically in tryptic soy media at 30°C. Genomic DNA was isolated using  
117 Wizard Miniprep kit (Promega, Madison, Wisconsin, USA). Library was constructed using Truseq  
118 DNA sample prep kit. Paired end sequence reads (101-nt) were obtained using Illumina HiSeq  
119 2000 platform (San Diego, California, USA) at National Instrumentation Center for Environment  
120 Management, Seoul National University (Seoul, Republic of Korea). Through sample multiplexing,  
121 sequencing reads from all thirteen libraries were obtained from a single run.

### 122 **Pretreatment of sequence reads and *de novo* assembly**

123 Trimmomatic (22) included in the A5-Miseq package (23) version 20140604 was used for adaptor  
124 sequence removal and quality trimming using modified parameters (SLIDINGWINDOW:4:20  
125 MINLEN:75) to obtain longer sequences. SGA (24) version 0.10.13 was used for k-mer-based error  
126 correction when required. For k-mer abundance analysis, Jellyfish (14) version 2.2.3 or khmer (16)  
127 version 2.0 was used with a k-mer size of 20. Jellyfish, a k-mer counting program without filtering  
128 function, runs much faster than khmer but gives similar results. Therefore, Jellyfish was used for  
129 the initial screen while khmer was used to filter out k-mers below a specified coverage of  
130 problematic reads or for counting, format conversion, and general manipulation of paired fastq files  
131 such as interleaving and splitting. CLC Genomics Workbench versions 8.5 or 9.0 was used for *de*  
132 *novo* assembly with a word size of 64. Trimming (low quality limit 0.01, max 1 ambiguous  
133 nucleotide allowed per read, min length 50 nucleotides) was applied in case trimmomatic was  
134 skipped. Subsampling prior to assembly was also carried out in the same environment (i.e., CLC  
135 Genomics Workbench). Average read coverages of contigs were obtained by selecting mapping  
136 options from the *de novo* assembly tool in CLC Genomics Workbench. Contig comparison and  
137 visualization of assembly metrics were carried out using QUAST (25) version 2.3. Prokka (26)  
138 version 1.11 was then run for functional annotation of assembled genome sequences. Nucleotide  
139 and amino acid sequences of predicted genes were analyzed using specI (27) to identify species.

140 **Identification of 16S rRNA genes**

141 Pairs of read files without pretreatment were converted to FASTA format and passed to REAGO  
142 (28) version 1.1 to retrieve reads originating from 16S rRNA genes and to reconstruct them  
143 separately (either from multiple copies of genes within a single strain or from contaminating  
144 genomes). The reconstructed 16S rRNA genes from REAGO (full genes only) and Prokka (full and  
145 partial genes) were analyzed using EzTaxon server (29).

146 **Estimation of contamination using metagenome analysis tools**

147 To estimate the proportion of contaminated reads and identify the source organism at various  
148 phylogenetic levels, a couple of tools for metagenomics sequence analysis were applied. Raw reads  
149 without pretreatment were subjected to analysis with MetaPhyler (30) SRV0.115, an optimized

150 version suitable for short reads, and to Kraken (31) version 0.10.5-beta using MiniKraken  
151 20141208 as the reference genome database. They were also subjected to analysis with PhyloSift  
152 (32) version 1.0.0\_01. Results were visualized using Krona (33). Kraken differs from the other two  
153 software in that it assigns taxonomic labels to each reads, whereas MetaPhyler and PhyloSift  
154 generate taxonomic profiles and phylogenetic analysis, respectively.

155

156

## RESULTS

157

### 158 K-mer abundance profiles of test datasets

159 We prepared test dataset with various conditions that might affect *de novo* assemblies. We also  
160 counted their k-mer frequencies. Simulated reads with increased error rate showed much  
161 divergence at low k-mer frequencies (Fig. 1A). There was a combinatorial effect of sequential  
162 quality trimming and error correction of reads on k-mer distribution at low frequencies with data  
163 volume adjustment so that all treated reads could have the same amounts of final basepairs (Fig.  
164 1B). Interestingly, error rate and pretreatment did not appear to be the major factor affecting the  
165 assembly metrics if adequate sequencing coverage was ensured without contamination  
166 (Supplementary Table S1). Real sequencing reads from repeat-rich genome *Shigella boydii*  
167 produced as many as 443 contigs (4.53 Mb) due to the presence of hundreds of copies of insertion  
168 sequences which resulted in highly fragmentary assembly with a shoulder peak just beyond the  
169 main one, representing k-mers from repetitive sequences (Fig. 1C). Although *E. coli* BL21 also  
170 showed multiple peaks at high frequency k-mer range, the relative height of the highest secondary  
171 peak to the main was only 0.23%. It was 45.3% for *Shigella boydii*.

172 Contamination appeared to be the major factor that deteriorated both assembly results and k-  
173 mer profiles (Fig. 1D). There was a secondary peak in the low frequency range with different peak  
174 locations and heights. We also carried out *de novo* assemblies with various contamination levels.  
175 Compared to species level contamination where 5-10% contamination mostly spoiled the  
176 assemblies, strain level contamination resulted in the worst assembly when 50% mixture was used  
177 (Supplementary Table S1 and Fig. S1). For the latter situation, k-mer spectrum is shown in Fig. 1E.  
178 It is reminiscent of a *de novo* assembly of a heterozygous diploid genome. We also compared k-mer  
179 spectra of simulated reads of haploid yeast *Saccharomyces cerevisiae* S288c and heterozygous  
180 diploid yeast *Candida albicans* SC5314 (Fig. 1F). Reads from haploid genome showed a major  
181 peak around sequencing depth (100x) and minor peaks arising from repeats at high frequencies. On  
182 the contrary, SC5314 showed the largest secondary peak left to the main peak. As expected,

183 heterozygous diploid genome resulted in much worse assembly than haploid genome  
184 (Supplementary Table S1).

185 **Bad assemblies from real data were associated with anomalous k-mer abundant profile**

186 Real Illumina sequencing data produced from one single multiplexed run of thirteen bacterial  
187 isolate genomes were preprocessed (trimming only) and assembled using CLC Genomics  
188 Assembler. At first glance, samples Bc1 and Bp1 failed in *de novo* assembly as they showed  
189 extraordinarily high contig numbers. In addition, the total contig lengths were much larger than the  
190 expected genome size (Table 1). Although Sample Bc2 resulted in a moderately large contig  
191 number that might be regarded as normal, it should be regarded as a failure due to total contig  
192 length of nearly 9.3 Mb, which is impossible for a *Bacillus cereus* strain. All reads were pretreated  
193 using trimmomatic (adaptor removal and trimming) and subjected to Jellyfish analysis for k-mer  
194 counting. As expected, samples Bc1, Bc2, and Bp1 all showed a secondary peak at the rare k-mer  
195 range (Fig. 2).

196 **Sample Bp1 was contaminated by a GC-rich genome**

197 While inspecting QUAST report for graphical representation of assembly results, we found that  
198 Bp1 contained contigs whose %GC was much higher (~70% on average) than what was expected  
199 for a *Bacillus pumilus* genome (Supplementary Fig. S2A). Contigs could be divided at 55% G+C  
200 into a low-GC group (172 contigs, total length of 3,759,031 bp, N50 of 906,842 bp) and a high-GC  
201 group (3,466 contigs, total length of 3,364,341 bp, N50 of 1,280 bp). BLAST analysis of the largest  
202 contig (17,311 bp) of the second group revealed that the high GC contigs originated from GC-rich  
203 *Caulobacter* species. GC-rich contamination in sample Bp1 was not conspicuous at the read level  
204 (Supplementary Fig. 2B) because only 2.91% of total reads were  $\geq$  55% G+C.

205 **Read subsampling or removing low-abundant k-mers improved *de novo* assemblies**

206 As a fast measure to improve the problem in assembly, reads were subsampled at 5-50% ranges and  
207 subject to *de novo* assembly. 5% of subsample yielded far better assemblies than using the whole  
208 dataset for Bc1 and Bp1 (Fig. 3). Based on k-mer spectrum analysis, the atypical peak at low k-mer  
209 frequencies disappeared gradually with decreasing subsample size. The shortcoming of this

210 treatment is the difficulty in choosing the proper sample size to abolish most reads containing low-  
211 abundant k-mers (probably due to contamination) while keeping adequate sequencing depth. When  
212 the total contig size calculated from the assembly of filtered reads, a better estimate for genome  
213 size, was used for the calculation of sequencing depth of subsamples, 5% of reads corresponded to  
214 31.7x (Bc2) or 48.7x (Bp1) coverages. These are slightly under the optimal level to ensure  
215 successful assemblies. A still better solution was to perform assembly after read filtering under a  
216 specified k-mer coverage (50 for Bc1 and Bp1; 100 for Bc1). This produced as little as 30 contigs.  
217 However, Bc2 assembly was not improved using subsampling or k-mer filtering because the two k-  
218 mer peaks significantly overlapped with each other.

219 **High contig numbers of failed assemblies were due to short and low-coverage contigs**

220 Cumulative contig length reached a plateau as short contigs were added (Fig. 4A), implying that  
221 longer contigs contributed the most to the total length. However, in failed assemblies with  
222 extraordinarily high contig numbers such as Bc1 and Bp1, short contigs accounted for half of the  
223 total contig length (Fig. 4B). Next, we plotted average read coverage, length, and cumulative length  
224 of contigs sorted in the increasing order of read coverage (Fig. 5). Normal assemblies showed  
225 similar pattern to Bp2, where an average read coverage leap (designated by two dashed lines)  
226 divided contigs into two groups. High coverage contigs contained sequences present once or more  
227 (repeats) that could be expected at a given sequencing depth. Contigs belonging to the low  
228 coverage group were very short (mostly < 1 kb). They contributed less to the total contig length in  
229 normal assemblies. For Bc1 and Bp1, short contigs with low coverage accounted for the majority  
230 of contig numbers. Quite high numbers of reads were mapped to low coverage contigs for poor  
231 assemblies, such as 1.5% for Bc1, 15.0% for Bc2, and 1.1% for Bp1. In normal assemblies, only  
232 1,132 – 5,696 reads out of tens of million reads were mapped to low coverage contigs  
233 (Supplementary Table S2). Total length of low coverage contigs were also very long (3.45 – 5.21  
234 Mb) for sample Bc1, Bc2, and Bp1. It was noteworthy that Bc2 had contigs with mid-level  
235 coverage. Their lengths were comparable to those in the high coverage group (Fig. 5). In contrast to  
236 Bc1 and Bp1, the low-to-mid level coverage group of Bc2 could be regarded as a high level of

237 assembly (Supplementary Table S3). However, we could not designate any single species to it  
238 because neither 16S rRNA gene sequence nor definitive specI analysis result (78.11% average  
239 identity to *Bacillus* sp. 2\_A\_57\_CT2, GenBank ACWD01000000) was obtained. We also found  
240 that the *de novo* assembly of artificially contaminated test dataset of 100x Illumina reads from *E.*  
241 *coli* BL21 containing 5% *B. subtilis* ATCC 1028 reads showed similar pattern of length-coverage  
242 distribution as Bc1 and Bp1 (Supplementary Fig. S4). Out of 4,577 contigs, 4,475 contigs with  
243 total length of 1,327,810 bp had low coverage (under 50x). Re-mapping after assembly revealed  
244 that low coverage contigs had only 89,988 reads (1.9% of total reads), where 89,594 reads of them  
245 were derived from *B. subtilis* genome. This observation further supports that short and low-  
246 coverage contigs in failed assembly are due to contaminating reads.

247 **Identification of multiple 16S rRNA genes from reads and contigs**

248 Because it became apparent that contamination in sequence reads was the main factor causing a  
249 large number of small contigs with low coverage, eventually leading to spoiled assembly, we  
250 determined the identities of contaminant. When read files without pretreatment were analyzed  
251 using REAGO (requiring reads of a fixed length), multiple full-length 16S ribosomal RNA genes  
252 were found from eleven out of thirteen samples. Because REAGO could distinguish ribosomal  
253 gene copies from a single genome, all full-length 16S ribosomal RNA genes were searched against  
254 database using EzTaxon server. 16S rRNA genes either full or partial were also identified from  
255 Prokka annotation of assembled sequences, where 16S rRNA genes from a single species were  
256 normally found from overcollapsed contigs. Results are summarized in Table 2. We could not find  
257 contaminating 16S rRNA genes in full form from REAGO results. However, fragmented  
258 caulobacterial sequences were found from at least five samples.

259 Secondary 16S rRNA genes predicted by Prokka were found to belong to *Paenibacillus*  
260 *galcialis* and *Caulobacter mirabilis* (in Bc1 and Bp1, respectively). The presence of *Panibacillus*  
261 *glacialis* gene in sample Bc1 might reflect cross-contamination from sample Pg1. It should be noted  
262 that multiple samples, at least six, contained 16S rRNA gene sequence (partial or full) of  
263 *Caulobacter* species. However, no secondary 16S rRNA could be found from Bc2 using REAGO

264 or Prokka, despite the completeness of contigs originating from contamination.

265 **Use of metagenome analysis tools suggests that caulobacterial contamination might be  
266 prevalent across samples**

267 We applied MetaPhyler to all raw reads of the 13 samples to estimate the relative abundance of  
268 taxonomic units to rank phylum through genus. Results were compared at family level, the highest  
269 level where possible contamination across all samples could be maximally distinguishable (Table  
270 3). Family *Caulobacteraceae* was detected from nine samples, including all six samples containing  
271 caulobacterial 16S rRNA genes from prior analysis. The abundance of *Caulobacteraceae* was the  
272 highest in Bp1 (0.46%) (Supplementary Fig. S5 for Krona plot). In Bc1, the abundance of  
273 *Paenibacillaceae* was 0.07%. In Bc2, the abundances of *Listeriaceae* (order *Bacillales*) and  
274 *Streptococcaceae* (order *Lactobacillales*) were 0.16% and 0.04%, respectively. Unexpectedly, in  
275 samples Bm1 and Bm2, the abundance of *Staphylococcaceae* and *Listeriaceae* (all order *Bacillales*)  
276 was about 0.2%. It was also notable that Pan and Pgl belonging to genus *Paenibacillus* contained a  
277 significant amount of *Bacillus* reads (relative abundance of 6.44% and 3.55%, respectively).

278 We then used Kraken to attach taxonomic label to each read after classification, where the  
279 resultant figures cannot be directly comparable with those obtained through MataPhyler or  
280 PhyloSift. Read classification rates across samples were significantly different in Kraken results.  
281 For examples, the classification rate was as high as 86.0% for Bs1 reads. It was only 5.1% for Pan  
282 or 1.3% for Pgl. Because Kraken analysis depends on short exact alignments of reads on prebuilt  
283 genome library, its results are largely affected by the comprehensiveness of the library. Kraken  
284 reported much diverse and detailed phylogenetic distribution (due to possible contamination) than  
285 MetaPhyler (Supplementary Fig. S6 for Bp1). However, the actual percentage for reads classified  
286 to irrelevant taxons was below 0.1%, making it difficult to discriminate real contamination from  
287 noise that might be a function of reference database. In particular, proteobacterial reads appeared to  
288 be prevalent among all samples, where *Alcaligenaceae* (*Achromobacter xylosoxidans*) and  
289 *Alteromonadaceae* (*Alteromonas mediterranea*) were the most common with a fairly similar  
290 proportion (Supplementary Fig. S7 for Bpf and Pan). Similar patterns were frequently found from

291 Kraken analyses of Illumina reads derived from other totally unrelated sequencing projects (the  
292 ratio of *Achromobacter xylosoxidans* to *Alteromonas mediterranea* was approximately 1:1~10:1,  
293 data not shown). Therefore, similar proteobacterial distribution patterns across multiple samples  
294 (except for caulobacterial contamination) without 16S rRNA evidence were likely to be false  
295 positives.

296 Finally, all reads were subjected to PhyloSift analysis, a phylogeny-driven statistical hypothesis  
297 test to determine the presence of phylogenetic lineages where abundance information is given as  
298 probability distribution. PhyloSift showed the most conservative results among the three analysis  
299 tools (i.e., MetaPhyler, Kraken, and PhyloSift). PhyloSift analysis results revealed that  
300 contaminations occurred only in Bc1, Bc2, Bp1, Pan and Pgl (Fig. 6).

301 ***De novo* assemblies of all samples were significantly improved after k-mer abundance  
302 filtering**

303 We previously showed that read filtration based on k-mer abundance could improve *de novo*  
304 assembly of samples Bc1 and Bp1 by removing less-abundant reads originating from  
305 contamination. Further comprehensive analyses revealed that nearly all samples had contamination  
306 at different levels. Except for Bc2 whose secondary peak in k-mer spectrum was not far enough  
307 from the main one to determine a suitable coverage cutoff, all twelve samples were filtered at k-  
308 mer abundance of 50 and subjected to *de novo* assembly. As shown in Fig. 7, the assemblies for all  
309 samples were greatly improved in terms of contig numbers. Because short and low-coverage  
310 contigs were not formed after filtering out those low-frequency reads, there was no significant loss  
311 in total contig length or N50 length.

312

313

## DISCUSSION

314

315 In this study, we took a systematic approach to determine the cause of failed Illumina assembly of  
316 bacterial genomes. Counting k-mers in sequencing reads with visualization was chosen as a quick  
317 and efficient method for the diagnosis of sequence reads. Sequencing error itself was not a crucial  
318 factor for successful *de novo* assembly as pretreatment such as trimming and error correction did  
319 not improve the results when sufficient sequencing depth, e.g., 100x, was ensured. Analyses using  
320 test datasets showed that the presence of repeats, contamination, and heterozygosity were the main  
321 reasons leading to poor Illumina assemblies for microbial genomes, which accompany minor peaks  
322 for k-mer abundance distribution.

323 At the first glance at assembly results, three (Bc1, Bc2, and Bp1) out of thirteen samples  
324 appeared to be problematic in terms of contig number and total contig length. In particular, Bc1 and  
325 Bp1 produced thousands of contigs whose total length were 3.9-5.0 Mb, which were larger than we  
326 expected. Coverage-length analysis showed that these contigs were divided into two groups based  
327 on average read coverage. The borderline of which was sequencing depth. The low-coverage  
328 contigs were usually short (< 1,000 kb). These short and low-coverage contigs comprised most of  
329 the contigs in the Bc1 and Bp1 assemblies. Re-mapping analysis indicated that reads responsible  
330 for the generation of short and low-coverage contigs ranged from 1.1% (Bp1) to 15.0% (Bc2) of  
331 total reads used. However, these numbers were negligible for other normal assemblies. This does  
332 not mean that contamination as low as ~1% of total reads is sufficient to spoil a *de novo* assembly.  
333 For example, only 1.9% of contaminating reads were mapped to short contigs when *E. coli* test  
334 dataset containing 5% *B. subtilis* reads were used. The remaining ~3% were unmapped, leaving  
335 only 3,347 reads (0.07% of total reads) mapped to high-coverage contigs.

336 K-mer spectra from real dataset leading to failed assemblies were very similar to those of test  
337 dataset with contamination. We could identify the source of contamination and estimate their  
338 proportions using several tools originally designed for metagenomics sequence analysis. Besides  
339 for specific contamination for individual samples (Bc1, Bc2, Bp1, Pan and Pgl), we unexpectedly

340 found that all thirteen samples belonging to *Firmicutes* (*Bacillus* or *Paenibacillus* strains) had  
341 proteobacterial sequences. This does not imply true contamination across all samples, while the  
342 presence of caulobacterial reads were evident from our analysis results.

343 It is evident that contamination could cause difficulties in *de novo* assemblies or mislead  
344 conclusions. A tool for contamination removal called DeConSeq (34) has been introduced, but it  
345 cannot be used for unknown contaminants because it depends on alignment to known reference  
346 sequences. This tool is only useful for removing host sequences from metagenomics samples.  
347 Merchant *et al.* have reported cross-species contamination from public genome sequences (*Bos*  
348 *Taurus* and *Neisseria gonorrhoeae* TCDC-NG08107) using Kraken system (35). However, they did  
349 not suggest any possible contamination source other than erroneously labelled DNA. Recently,  
350 Mukherjee *et al.* have reported that PhiX sequence frequently used for a control during Illumina  
351 sequencing could be the source of contamination by screening publicly available microbial isolate  
352 genome sequences (36).

353 Then, what would be the cause of contamination in high-throughput genome sequencing  
354 experiments? In most cases, contamination could be due to insufficient axenic culture techniques of  
355 careless experimenters. Sometimes, bacterial stocks available from culture collections may be  
356 already contaminated. Simultaneous manipulation of multiple samples can also cause cross-  
357 contamination between samples. However, we suspect that the contamination with identical species,  
358 totally irrelevant to the laboratory environment, across multiple samples might have occurred  
359 during or after sequencing library preparation. Furthermore, bacterial cultivation and DNA  
360 preparation steps were undertaken at three independent laboratories in this study.

361 Insufficient wash between sequencing runs might cause carry-over contamination  
362 (<http://seqanswers.com/forums/showthread.php?t=29110>). In such a case, reads from a particular  
363 sample from the previous run could appear in the result of current sample whose barcode is  
364 coincident. In our results, however, multiple samples with different barcode showed similar  
365 patterns of contamination. It implies that contamination might have occurred during the library  
366 construction step at the sequencing facility. Very recently, we came across 1% archaeal reads and

367 6% eukaryotic reads from a myxobacterial sequencing result produced by the largest domestic  
368 sequencing company. Contamination caused by sequencing service provider poses a serious  
369 problem for the reliability of data, because it is very difficult for customers to take proper measures.

370 Not all contaminations are represented by anomalies in k-mer frequency distribution. We found  
371 that distinguishable k-mer frequency distribution could be hardly detected from simulated test  
372 dataset when contamination was 1% or less (data not shown). We cannot suggest any reference  
373 values for percent contamination that can ensure successful assembly. This can vary with actual  
374 situations. For example, 1% contamination can spoil assembly, while 5% contamination can  
375 generate reasonable assembly unless the contamination is dominated by one organism. However,  
376 there are a couple of things that we can consider, including diversity in contamination, sequence  
377 similarity between target organism and the contaminants, and sequencing quality. Even the choice  
378 of assembly program with a specific parameter set can greatly affect assembly results. Thus, as a  
379 general guideline, we propose to filter reads at a particular k-mer frequency (a quarter of  
380 sequencing depth would be suitable) for *de novo* assembly of microbial isolate genomes, even if  
381 contamination is not evident after the initial diagnosis using Jellyfish. Selecting contigs after the  
382 assembly step based on coverage would serve the same purpose. Read classification tools could  
383 then be applied for raw reads for deeper analysis of contamination, although they take long running  
384 time with the exception of MetaPhyler.

385 In summary, contamination is no longer a problem specific to individual samples in  
386 contemporary high-throughput sequencing era. Although not all incidence of contamination is  
387 reflected by unusual assembly metric values, a systematic analysis can reveal the underlying  
388 problem throughout samples. Our experience might provide insights on the utility of raw  
389 sequencing data for quality assessment of draft genome assemblies.

390

391

## ACKNOWLEDGMENTS

392

393 We thank Tai-Boong Uhm (Chonbuk National University, Republic of Korea) and Yoav Bashan  
394 (The Bashan Institute of Science, USA) for providing bacterial strains for sequencing. We also  
395 thank Young Mi Sim (Korean Bioinformation Center) for technical assistance. This work was  
396 supported by KRIBB Research Initiative Program (KGM2111622) and the Bio & Medical  
397 Technology Development Program (NRF-2010-0029345) funded by Ministry of Science, ICT, and  
398 Future Planning, Republic of Korea.

399

400

## REFERENCES

401

- 402 1. **Loman NJ, Pallen MJ.** 2015. Twenty years of bacterial genome sequencing. *Nat Rev Microbiol* **13**:787-794.
- 403 2. **Pop M, Salzberg SL.** 2008. Bioinformatics challenges of new sequencing technology. *Trends Genet* **24**:142-149.
- 404 3. **El-Metwally S, Hamza T, Zakaria M, Helmy M.** 2013. Next-generation sequence assembly: four stages of data processing and computational challenges. *PLoS Comput Biol* **9**:e1003345.
- 405 4. **Birney E.** 2011. Assemblies: the good, the bad, the ugly. *Nat Methods* **8**:59-60.
- 406 5. **Junemann S, Prior K, Albersmeier A, Albaum S, Kalinowski J, Goesmann A, Stoye J, Harmsen D.** 2014. GABenchToB: a genome assembly benchmark tuned on bacteria and benchtop sequencers. *PLoS One* **9**:e107014.
- 407 6. **Magoc T, Pabinger S, Canzar S, Liu X, Su Q, Puiu D, Tallon LJ, Salzberg SL.** 2013. GAGE-B: an evaluation of genome assemblers for bacterial organisms. *Bioinformatics* **29**:1718-1725.
- 408 7. **Koren S, Treangen TJ, Hill CM, Pop M, Phillippy AM.** 2014. Automated ensemble assembly and validation of microbial genomes. *BMC Bioinformatics* **15**:126.
- 409 8. **Liao YC, Lin HH, Sabharwal A, Haase EM, Scannapieco FA.** 2015. MyPro: a seamless pipeline for automated prokaryotic genome assembly and annotation. *J Microbiol Methods* **113**:72-74.
- 410 9. **Koren S, Phillippy AM.** 2015. One chromosome, one contig: complete microbial genomes from long-read sequencing and assembly. *Curr Opin Microbiol* **23**:110-120.
- 411 10. **Chin CS, Alexander DH, Marks P, Klammer AA, Drake J, Heiner C, Clum A, Copeland A, Huddleston J, Eichler EE, Turner SW, Korlach J.** 2013. Nonhybrid, finished microbial genome assemblies from long-read SMRT sequencing data. *Nat Methods* **10**:563-569.
- 412 11. **Liao YC, Lin SH, Lin HH.** 2015. Completing bacterial genome assemblies: strategy and performance comparisons. *Sci Rep* **5**:8747.
- 413 12. **Zerbino DR, Birney E.** 2008. Velvet: algorithms for de novo short read assembly using de Bruijn graphs. *Genome Res* **18**:821-829.
- 414 13. **Alkan C, Sajjadian S, Eichler EE.** 2011. Limitations of next-generation genome sequence assembly. *Nat Methods* **8**:61-65.
- 415 14. **Marcais G, Kingsford C.** 2011. A fast, lock-free approach for efficient parallel counting of occurrences of k-mers. *Bioinformatics* **27**:764-770.
- 416 15. **Anvar SY, Khachatryan L, Vermaat M, van Galen M, Pulyakhina I, Ariyurek Y, Kraaijeveld K, den Dunnen JT, de Knijff P, t Hoen PA, Laros JF.** 2014. Determining the quality and complexity of next-generation sequencing data without a reference genome. *Genome Biol* **15**:555.
- 417 16. **Crusoe MR, Alamdin HF, Awad S, Boucher E, Caldwell A, Cartwright R, Charbonneau A, Constantinides B, Edvenson G, Fay S, Fenton J, Fenzl T, Fish J, Garcia-Gutierrez L, Garland P, Gluck J, Gonzalez I, Guermond S, Guo J, Gupta A, Herr JR, Howe A, Hyer A, Harpfer A, Irber L, Kidd R, Lin D, Lippi J, Mansour T, McA'Nulty P, McDonald E, Mizzi J, Murray KD,**

- 438                   **Nahum JR, Nanlohy K, Nederbragt AJ, Ortiz-Zuazaga H, Ory J, Pell J, Pepe-Ranney C, Russ**  
439                   **ZN, Schwarz E, Scott C, Seaman J, Sievert S, Simpson J, Skennerton CT, Spencer J,**  
440                   **Srinivasan R, Standage D, Stapleton JA, Steinman SR, Stein J, Taylor B, Trimble W, Wiencko**  
441                   **HL, Wright M, Wyss B, Zhang Q, Zyme E, Brown CT.** 2015. The khmer software package:  
442                   enabling efficient nucleotide sequence analysis. *F1000Res* **4**:900.
- 443     17.           **Jeong H, Kim HJ, Lee SJ.** 2015. Complete genome sequence of *Escherichia coli* strain BL21.  
444                   Genome Announc **3**:e00134-00115.
- 445     18.           **Jeong H, Sim YM, Park SH, Choi SK.** 2015. Complete genome sequence of *Bacillus subtilis*  
446                   strain ATCC 6051a, a potential host for high-level secretion of industrial enzymes. *Genome*  
447                   Announc **3**:e00532-00515.
- 448     19.           **Jeong H, Lee DH, Ryu CM, Park SH.** 2016. Toward complete bacterial genome sequencing  
449                   through the combined use of multiple next-generation sequencing platforms. *J Microbiol Biotechnol*  
450                   **26**:207-212.
- 451     20.           **Huang W, Li L, Myers JR, Marth GT.** 2012. ART: a next-generation sequencing read simulator.  
452                   *Bioinformatics* **28**:593-594.
- 453     21.           **Kim YS, Jeong JO, Cho SH, Jeong DY, Uhm T-B.** 2012. Antimicrobial and biogenic amine-  
454                   degrading activity of *Bacillus licheniformis* SCK B11 isolated from traditionally fermented red  
455                   pepper paste. *Kor J Microbiol* **48**:163-170.
- 456     22.           **Bolger AM, Lohse M, Usadel B.** 2014. Trimmomatic: a flexible trimmer for Illumina sequence data.  
457                   *Bioinformatics* **30**:2114-2120.
- 458     23.           **Coil D, Jospin G, Darling AE.** 2015. A5-miseq: an updated pipeline to assemble microbial  
459                   genomes from Illumina MiSeq data. *Bioinformatics* **31**:587-589.
- 460     24.           **Simpson JT, Durbin R.** 2010. Efficient construction of an assembly string graph using the FM-  
461                   index. *Bioinformatics* **26**:i367-373.
- 462     25.           **Gurevich A, Saveliev V, Vyahhi N, Tesler G.** 2013. QUAST: quality assessment tool for genome  
463                   assemblies. *Bioinformatics* **29**:1072-1075.
- 464     26.           **Seemann T.** 2014. Prokka: rapid prokaryotic genome annotation. *Bioinformatics* **30**:2068-2069.
- 465     27.           **Mende DR, Sunagawa S, Zeller G, Bork P.** 2013. Accurate and universal delineation of  
466                   prokaryotic species. *Nat Methods* **10**:881-884.
- 467     28.           **Yuan C, Lei J, Cole J, Sun Y.** 2015. Reconstructing 16S rRNA genes in metagenomic data.  
468                   *Bioinformatics* **31**:i35-43.
- 469     29.           **Chun J, Lee JH, Jung Y, Kim M, Kim S, Kim BK, Lim YW.** 2007. EzTaxon: a web-based tool  
470                   for the identification of prokaryotes based on 16S ribosomal RNA gene sequences. *Int J Syst Evol*  
471                   Microbiol **57**:2259-2261.
- 472     30.           **Liu B, Gibbons T, Ghodsi M, Treangen T, Pop M.** 2011. Accurate and fast estimation of  
473                   taxonomic profiles from metagenomic shotgun sequences. *BMC Genomics* **12 Suppl 2**:S4.
- 474     31.           **Wood DE, Salzberg SL.** 2014. Kraken: ultrafast metagenomic sequence classification using exact  
475                   alignments. *Genome Biol* **15**:R46.
- 476     32.           **Darling AE, Jospin G, Lowe E, Matsen FA, Bik HM, Eisen JA.** 2014. PhyloSift: phylogenetic

- 477 analysis of genomes and metagenomes. PeerJ **2**:e243.
- 478 33. **Ondov BD, Bergman NH, Phillippy AM.** 2011. Interactive metagenomic visualization in a Web  
479 browser. BMC Bioinformatics **12**:385.
- 480 34. **Schmieder R, Edwards R.** 2011. Fast identification and removal of sequence contamination from  
481 genomic and metagenomic datasets. PLoS One **6**:e17288.
- 482 35. **Merchant S, Wood DE, Salzberg SL.** 2014. Unexpected cross-species contamination in genome  
483 sequencing projects. PeerJ **2**:e675.
- 484 36. **Mukherjee S, Huntemann M, Ivanova N, Kyrpides NC, Pati A.** 2015. Large-scale contamination  
485 of microbial isolate genomes by Illumina PhiX control. Stand Genomic Sci **10**:18.
- 486

487 **Table 1. List of bacterial strains and sequencing summary** (Pretreatments and *de novo* assembly were performed using CLC Genomics Workbench  
 488 version 8.5. Trim rates based on the number of reads ranged from 80.24% to 92.02%).

Sample ID	Strain description	Availability	No. of reads	No. of basepairs	No. of contigs <sup>a</sup>	Total contig length	N50
Bpf	“ <i>Bacillus polyfermenticus</i> ” Bpf	Lab collection	29,008,528	2,929,861,328	90 (63)	4,127,902	502,253
Bc1	<i>Bacillus cereus</i> ATCC 4342	ATCC	38,787,810	3,917,568,810	6,052 (4,312)	10,444,843	8,376
Bc2	<i>Bacillus cereus</i> ATCC 31382	ATCC	24,280,592	2,452,339,792	119 (56)	9,286,527	443,015
BaD11	<i>Bacillus licheniformis</i> SCK B11	T.-B. Um (21)	31,066,026	3,137,668,626	84 (51)	4,271,421	267,419
Bm1	<i>Bacillus megaterium</i> Bm1 <sup>b</sup>	Y. Bashan	26,594,682	2,686,062,882	133 (93)	5,279,131	1,118,798
Bm2	<i>Bacillus megaterium</i> Bm2 <sup>b</sup>	Y. Bashan	26,524,590	2,678,983,590	78 (52)	5,113,416	1,121,613
Bp1	<i>Bacillus pumilus</i> Bp1 <sup>b</sup>	Y. Bashan	43,302,480	4,373,550,480	3,638 (2,472)	7,123,372	61,549
Bp2	<i>Bacillus pumilus</i> Bp2 <sup>b</sup>	Y. Bashan	39,622,506	4,001,873,106	44 (33)	3,683,921	968,875
ES4	<i>Bacillus pumilus</i> ES4 <sup>b</sup>	Y. Bashan	29,157,078	2,944,864,878	69 (57)	3,695,884	969,001
Rizo	<i>Bacillus pumilus</i> Rizo <sup>b</sup>	Y. Bashan	39,163,182	3,955,481,382	191 (179)	3,743,083	968,988
Bsu	<i>Bacillus subtilis</i> Bsu <sup>b</sup>	Y. Bashan	23,086,814	2,331,768,214	64 (51)	4,078,262	1,055,276
Pan	<i>Paenibacillus antarcticus</i> KCTC 13016	KCTC	24,832,632	2,508,095,832	129 (95)	5,373,088	385,650
Pgl	<i>Paenibacillus glacialis</i> KCTC 13874	KCTC	41,997,612	4,241,758,812	177 (97)	5,714,841	217,285

489 <sup>a</sup> Numbers in parentheses designate the number of contigs shorter than 1,000 bp.

490 <sup>b</sup> Endophytic bacteria isolated from cacti.

491

492

493

494 **Table 2. Identification of 16S rRNA genes from reads or assemblies and their EzTaxon analysis results** (Copies of 16S rRNA genes identified by  
 495 REAGO for samples Bpf, Bc2, and Bs1 showed different top hits due to intragenomic variations. In such cases, results that were the most similar to Prokka  
 496 were chosen)

Sample ID	From REAGO results <sup>a</sup>	From Prokka results
Bpf	(2) <i>Bacillus siamensis</i> KCTC 13613(T) 99.87%	<i>Bacillus siamensis</i> KCTC 13613(T) 99.93%
Bc1	Not identified	<i>Bacillus anthracis</i> ATCC 14758(T) 100% (partial) <i>Paenibacillus glacialis</i> KGC91(T) 99.75%
Bc2	(6) <i>Bacillus subtilis</i> subsp. <i>inaquosorum</i> KCTC 13429(T) 99.93%	(partial) <i>Bacillus subtilis</i> subsp. <i>inaquosorum</i> KCTC 13429(T) 100%
BaD11	(7) <i>Bacillus licheniformis</i> ATCC 14580(T) 99.87% <sup>b</sup>	<i>Bacillus licheniformis</i> ATCC 14580(T) 99.93%
Bm1	(10) <i>Bacillus megaterium</i> NBRC 15308 99.74% <sup>b</sup>	<i>Bacillus aryabhattai</i> B8W22(T) 100% <sup>c</sup>
Bm2	(5) <i>Bacillus aryabhattai</i> B8W22(T) 99.87% <sup>b</sup>	<i>Bacillus aryabhattai</i> B8W22(T) 100%
Bp1	(2) <i>Bacillus safensis</i> FO-36b(T) 99.93%	<i>Bacillus safensis</i> FO-36b(T) 100% <i>Caulobacter mirabilis</i> FWC38(T) 97.39
ES4	(2) <i>Bacillus safensis</i> FO-36b(T) 100% <sup>b</sup>	<i>Bacillus safensis</i> FO-36b(T) 100%
Bp2	(2) <i>Bacillus safensis</i> FO-36b(T) 99.87% <sup>b</sup>	<i>Bacillus safensis</i> FO-37b(T) 100%
Rizo	Not identified	<i>Bacillus safensis</i> FO-36b(T) 100%
Bs1	(4) <i>Bacillus subtilis</i> subsp. <i>inaquosorum</i> KCTC 13429(T) 99.87%	<i>Bacillus subtilis</i> subsp. <i>inaquosorum</i> KCTC 13429(T) 99.93%
Pan	(2) <i>Paenibacillus antarcticus</i> LMG 22078(T) 100% -all	<i>Paenibacillus antarcticus</i> LMG 22078(T) 100%
Pgl	(8) <i>Paenibacillus glacialis</i> KFC91(T) 99.60%	<i>Paenibacillus glacialis</i> KFC91(T) 99.65%

497 <sup>a</sup>Numbers in parentheses indicate the number of full 16S rRNA gene identified using REAGO.

498 <sup>b</sup>Fragments of *Caulobacter mirabilis* FWC38(T) 16S rRNA genes were found.

499 <sup>c</sup>*Bacillus megaterium* NBRC 15308 (99.87%) ranked the secon

0 **Table 3. Results obtained from 13 sequence reads using metagenome analysis tools** (Results shown at family level, which was the highest taxonomy level that could  
 1 maximize the difference between samples. Asterisks represent samples that contain caulobacterial 16S rRNA genes. Numbers given by PhyloSift are summed taxonomic mass  
 2 distribution. Their ratios are available from Krona plot)

	Bpf	Bc1	Bc2	BaD11*	Bm1*	Bm2*	ES4*	Bp1*	Bp2*	Bsu	Pan	Pgl	Rizo	
<b>Summary</b>														
Laboratory	A	A	A	B	B	B	B	B	B	B	A	A	B	
Total number of reads	29,008,528	38,787,810	24,280,592	31,066,026	26,594,682	26,524,590	29,157,078	43,302,480	39,622,506	23,086,814	24,832,632	41,997,612	39,163,182	
MetaPhyler (# reads)	64,659	77,771	64,661	77,552	34,915	31,742	79,104	79,216	75,009	83,433	4,091	4,994	83,554	
Kraken (# reads)	22,812,318	29,763,422	19,231,872	26,189,384	20,097,293	16,433,313	6,045,238	8,925,429	8,184,870	19,858,356	1,257,652	545,962	8,089,394	
PhyloSift (probability)	104,418	173,893	109,780	155,672	122,118	126,832	154,933	231,923	201,438	124,361	70,090	135,006	209,387	
Metaphyler (% classified)	0.22%	0.20%	0.27%	0.25%	0.13%	0.12%	0.27%	0.18%	0.19%	0.36%	0.02%	0.01%	0.21%	
Kraken (% classified)	78.64%	76.73%	79.21%	84.30%	75.57%	61.96%	20.73%	20.61%	20.66%	86.02%	5.06%	1.30%	20.66%	
PhyloSift (%)	0.36%	0.45%	0.45%	0.50%	0.46%	0.48%	0.53%	0.54%	0.51%	0.54%	0.28%	0.32%	0.53%	
<b>MetaPhyler<sup>c</sup></b>														
<i>Bacillaceae</i>	99.52%	99.88%	99.25%	99.67%	97.53%	97.74%	99.81%	99.38%	99.82%	99.47%	6.44%	3.55%	99.81%	
<i>Paenibacillaceae</i>	0.01%	0.07%									91.66%	94.47%	0.00% (3) <sup>a</sup>	
<i>Staphylococcaceae</i>					0.15%	0.16%								
<i>Listeriaceae</i>				0.16%		0.04%	0.04%							
<i>Streptococcaceae</i>					0.04%									
<i>Proteobacteria</i> (phylum)				0.01%	0.07%	0.23%	0.1%	0.09%	0.56%	0.04%	0.06%		0.07%	
<i>Caulobacteraceae</i>	0.00% (2) <sup>a</sup>				0.03%	0.17%	0.07%	0.04%	0.46%	0.03%	0.03%		0.04%	
<b>Kraken<sup>c</sup></b>														
<i>Bacillaceae</i>	94.28%	99%	95.74%	99.35%	98.96%	99%	97.03%	96.35%	97.27%	99.2%	6.16%	14.57%	97.01%	
<i>Paenibacillaceae</i>		0.01%			0.02%			0.07%	0.08%	0.07%		9.49%	49.32%	0.07%
<i>Staphylococcaceae</i>			0.01%				0.01%	0.02%	0.02%				0.02%	
<i>Listeriaceae</i>				0.01%				0.05%	0.05%	0.05%			0.31%	0.05%
<i>Streptococcaceae</i>								0.02%	0.02%	0.02%			0.82%	0.02%
<i>Proteobacteria</i> (phylum)	5.01%	0.04%	0.16%	0.04%	0.08%	0.04%	0.41%	1.01%	0.37%	0.03%	75.56%	2.01%	0.35%	
<i>Alcaligenaceae</i>	0.82%	0.01%	0.01%		0.02%			0.04%	0.15%	0.05%		14.99%	0.27%	0.02%
<i>Alteromonadaceae</i>	4.18%	0.02%	0.14%	0.01%	0.02%	0.01%	0.2%	0.27%	0.2%	0.01%	61.36%	0.92%	0.14%	
<i>Burkholderiaceae</i>						0.01%	0.01%	0.02%	0.08%	0.01%				0.02%
<i>Caulobacteraceae</i>					0.01%	0.02%	0.01%	0.04%	0.23%	0.02%	0.01%			0.05%
<b>PhyloSift<sup>c</sup></b>														
<i>Bacillaceae</i>	94.90%	95.79%	89.64%	95.96%	94.22%	94.41%	94.84%	93.81%	95.05%	95.63%	2.24%	1.33%	94.98%	
<i>Paenibacillaceae</i>		1.52%									97.81%	97.97%		
<i>Streptococcaceae</i>				5.74%										
<i>Caulobacterales</i> (order <sup>b</sup> )									1.15%					

3 <sup>a</sup>Numbers in the parentheses indicate classified reads.

4 <sup>b</sup> Result at family level was not available.

5     <sup>c</sup> Percentages represent relative abundance (MetaPhyler), ratio of classified reads (Kraken), and ratio of probability mass distribution (PhyloSift).

506

## LIST OF FIGURES

507

508 **Fig. 1. Abundance profiles of 20-mers in test dataset.** Sequencing depth of all dataset are 100x  
509 unless otherwise mentioned. All axes are shown in log scale. A, Simulated and real reads  
510 from *E. coli* BL21 with different errors. B, Real reads from *B. subtilis* KCTC 1028 with  
511 either trimming or error correction. All reads were adjusted to 443x (final dataset). C, Real  
512 reads at 640x from repeat-rich genome of *Shigella boydii* ATCC 9210. D, *E. coli* BL21 reads  
513 contaminated with 5% or 10% *B. subtilis* KCTC 1028 reads. E, 50:50 mixture of simulated  
514 reads from *E. coli* K-12 MG1655 and real reads from *E. coli* BL21. F, Simulated reads from  
515 diploid yeast *Saccharomyces cerevisiae* S288c and heterozygous diploid yeast *Candida*  
516 *albicans* SC5314.

517 **Fig. 2. Abundance profiles of 20-mers in selected sequence reads.**

518 **Fig. 3. Effect of subsampling or filtration on de novo assembly.** A, Comparison of assembly  
519 results. B-D, Changes in k-mer distribution of reads caused by subsampling for Bp1, Bc1, or  
520 Bc1.

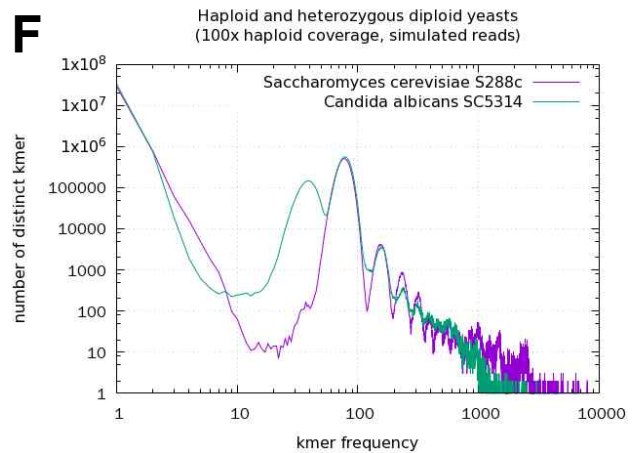
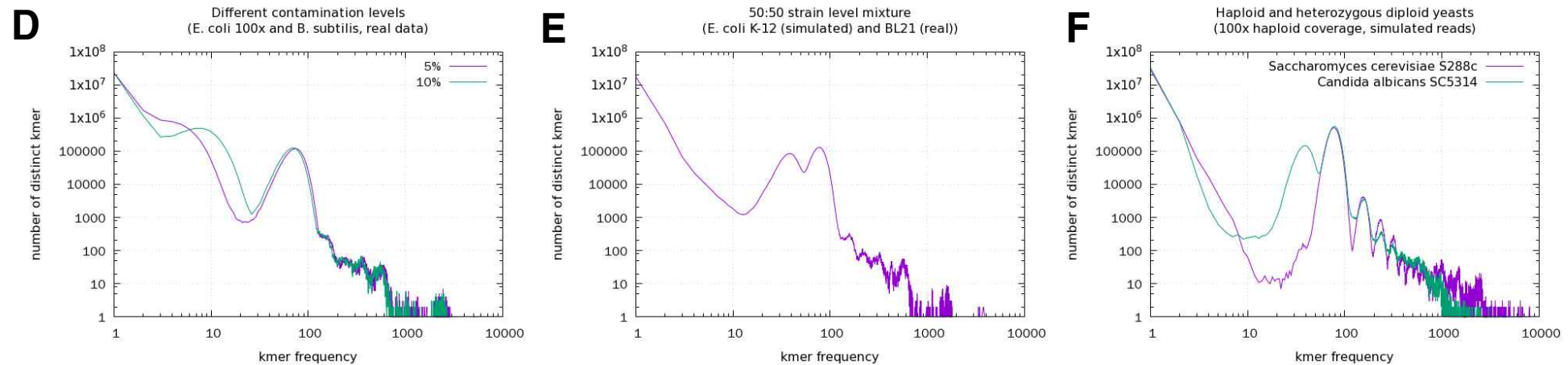
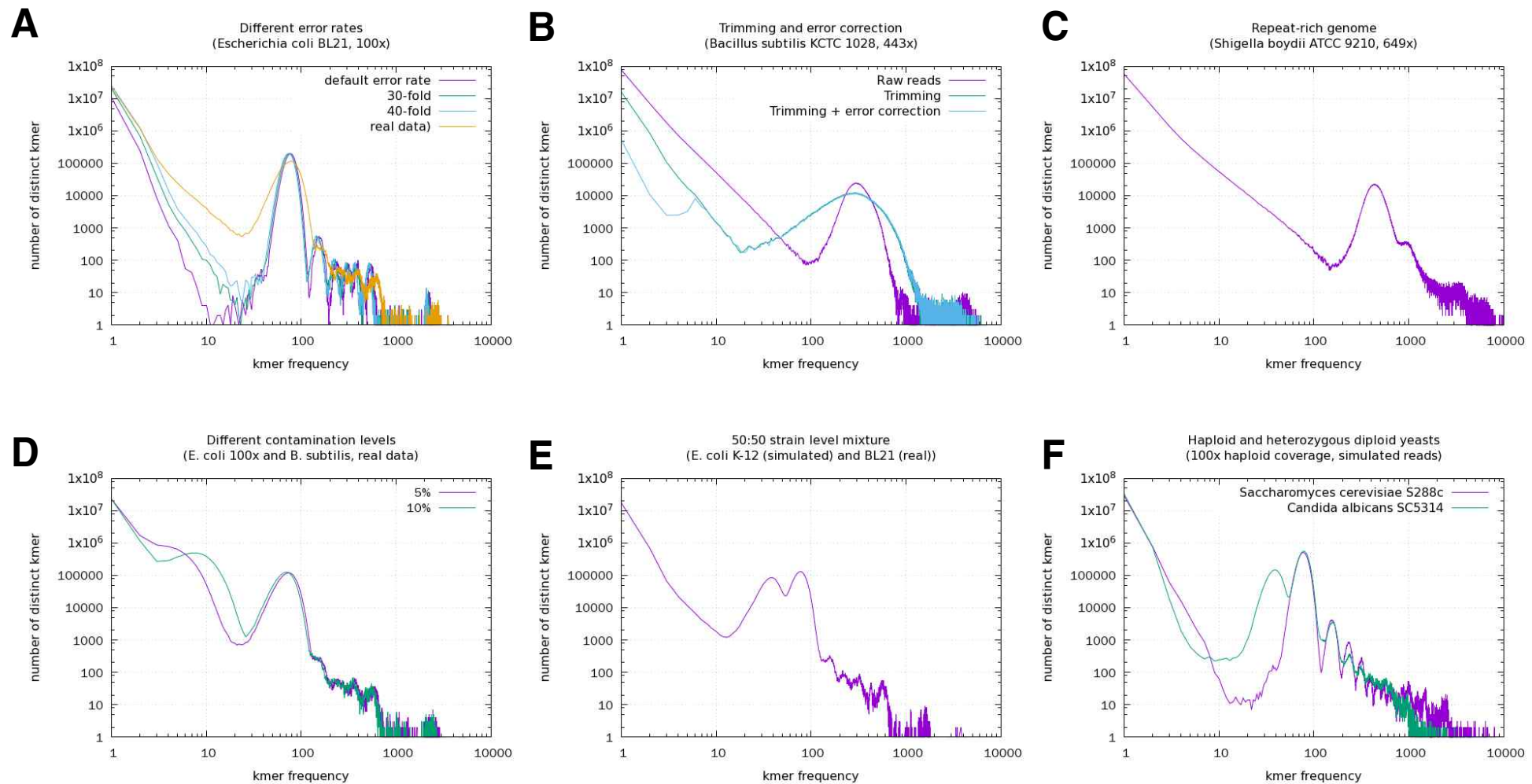
521 **Fig. 4. Cumulative length plot of reversely sorted contigs.** A, Eleven of the 13 samples (except  
522 Bc1 and Bp1). B, Plot for Bc1 and Bp1.

523 **Fig. 5. Coverage-length plot of assemblies.** Contigs are sorted in increasing order.

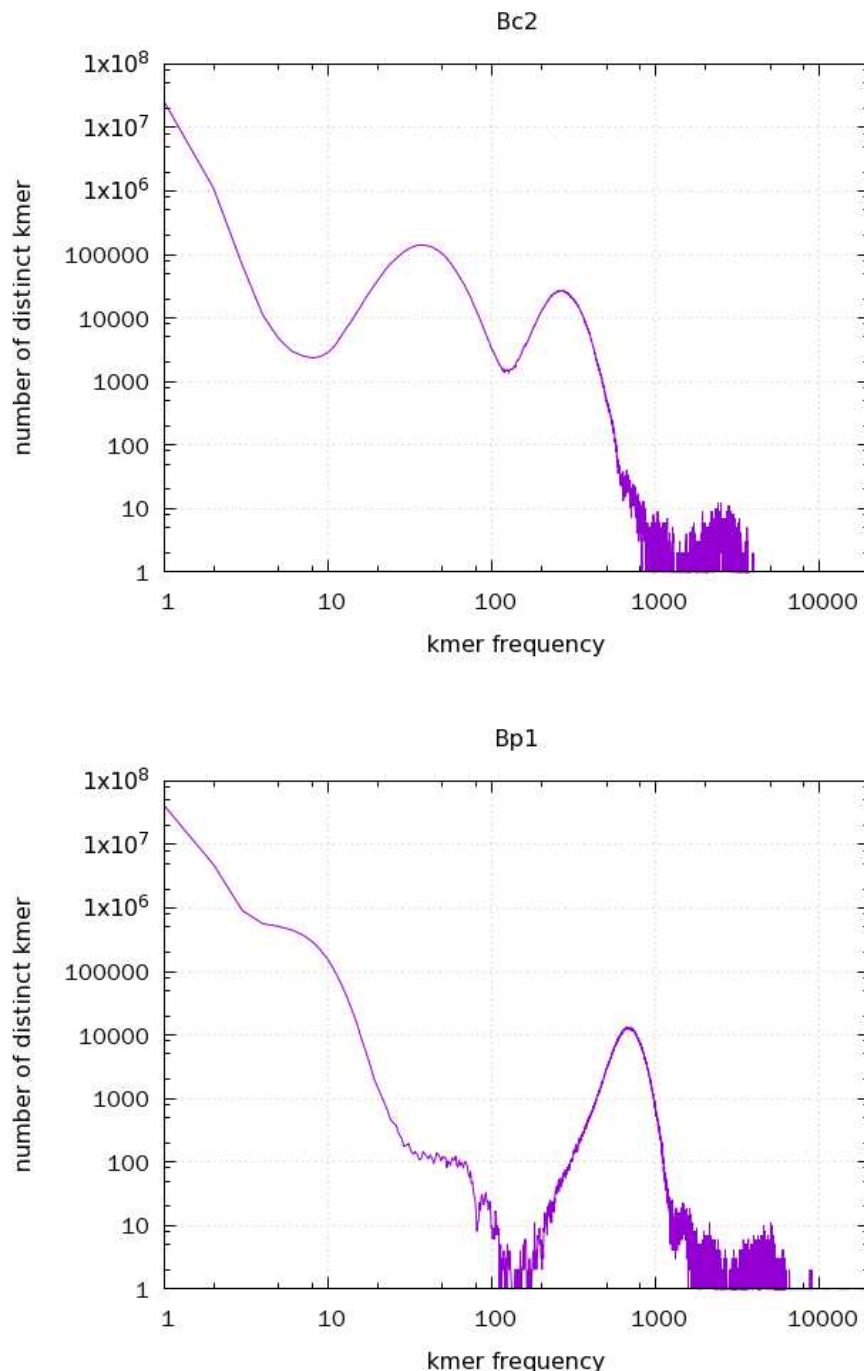
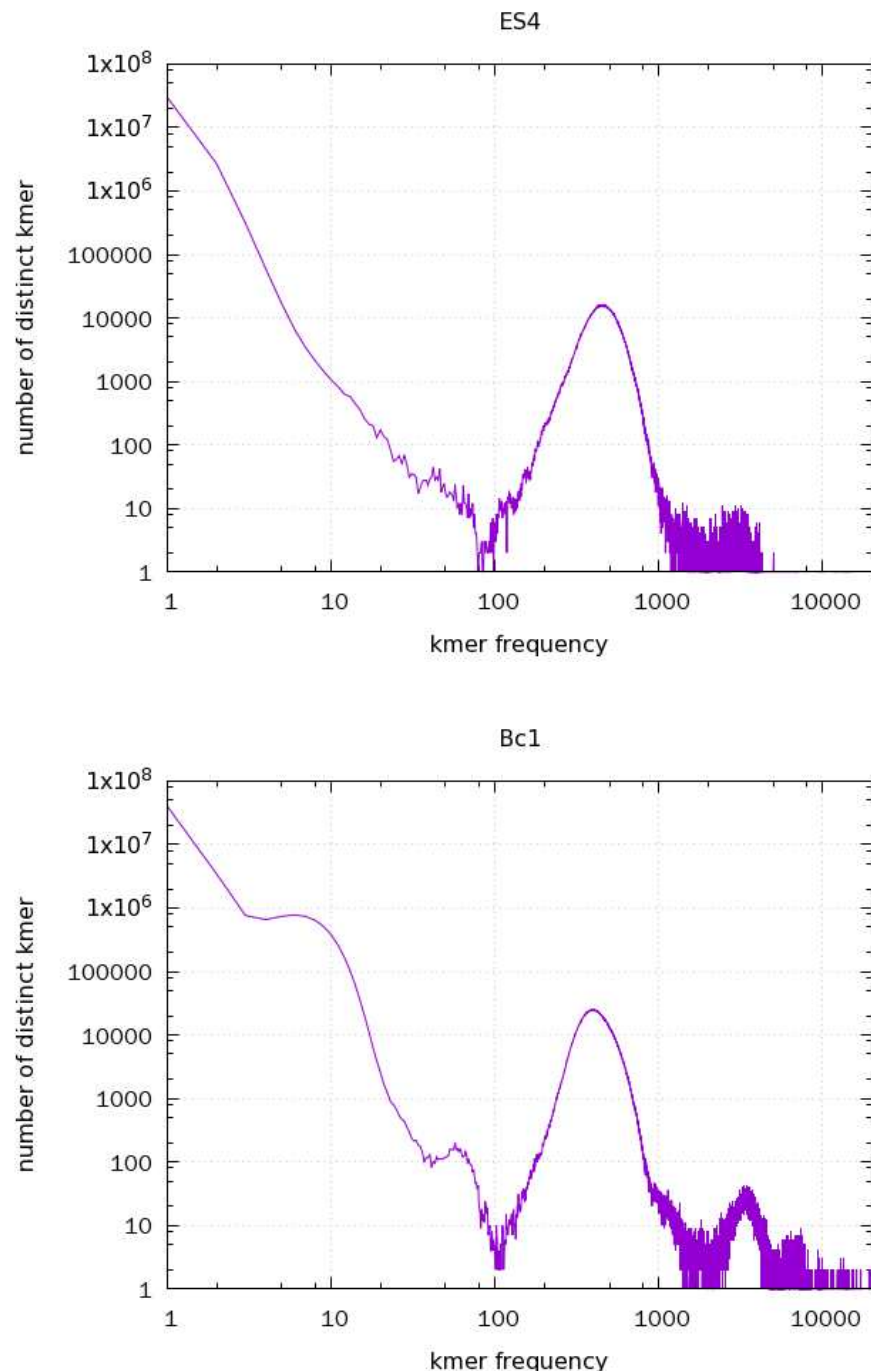
524 **Fig. 6. Krona plots of PhyloSift analysis results for selected samples Bc1, Bc2, and Pgl.**

525 **Fig. 7. De novo assembly results after k-mer filtering of reads for twelve of the 13 samples  
526 (except Bc2).**

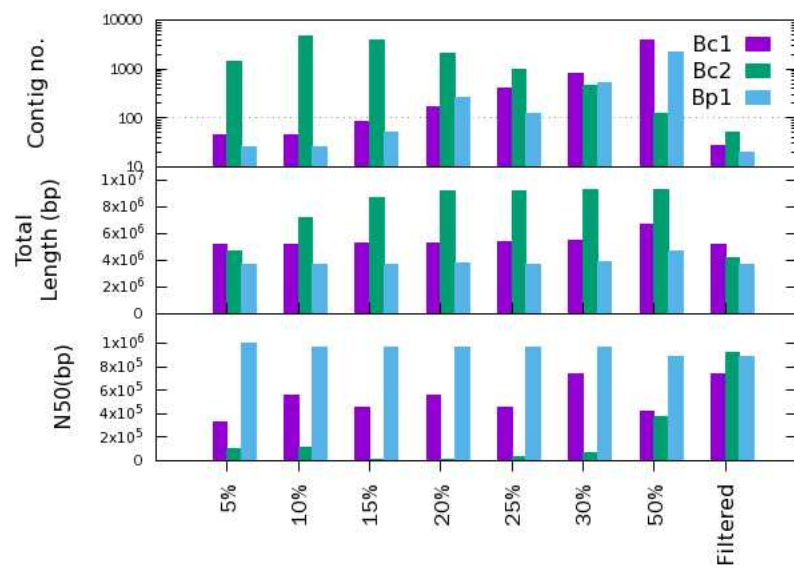
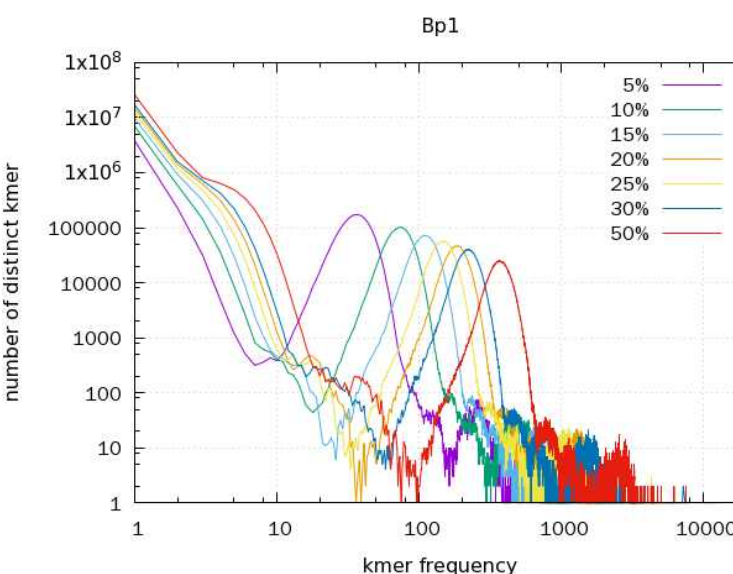
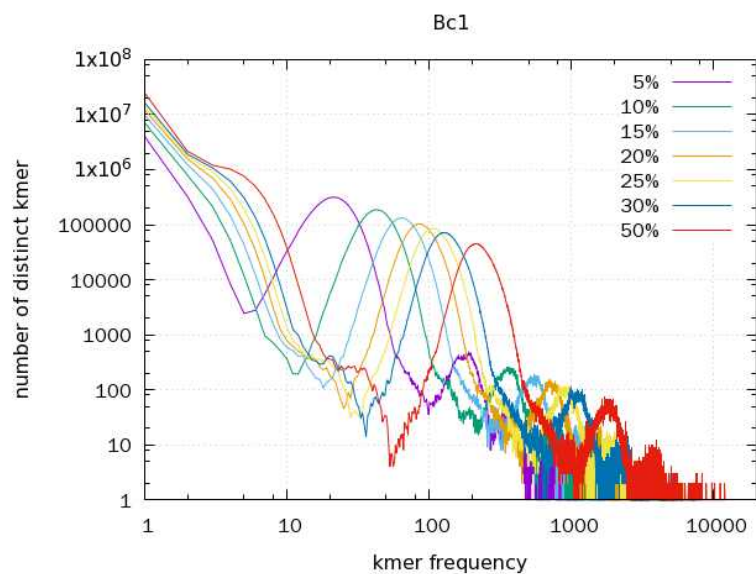
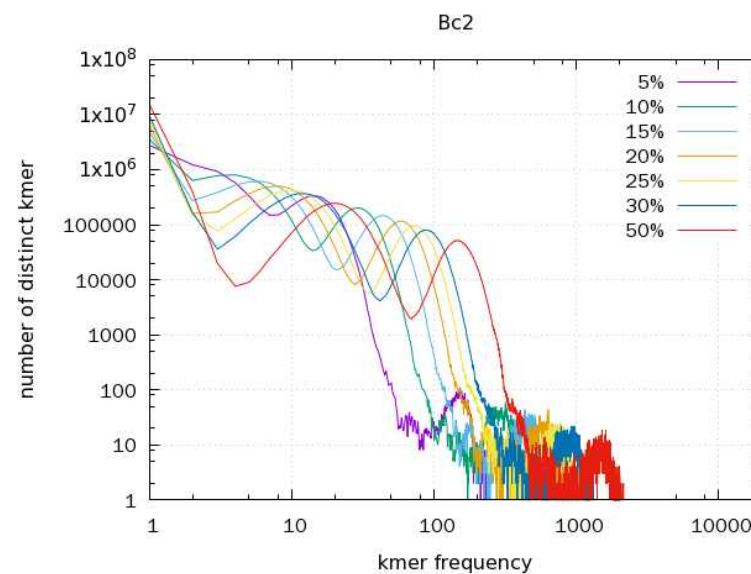
# Fig. 1



# Fig. 2

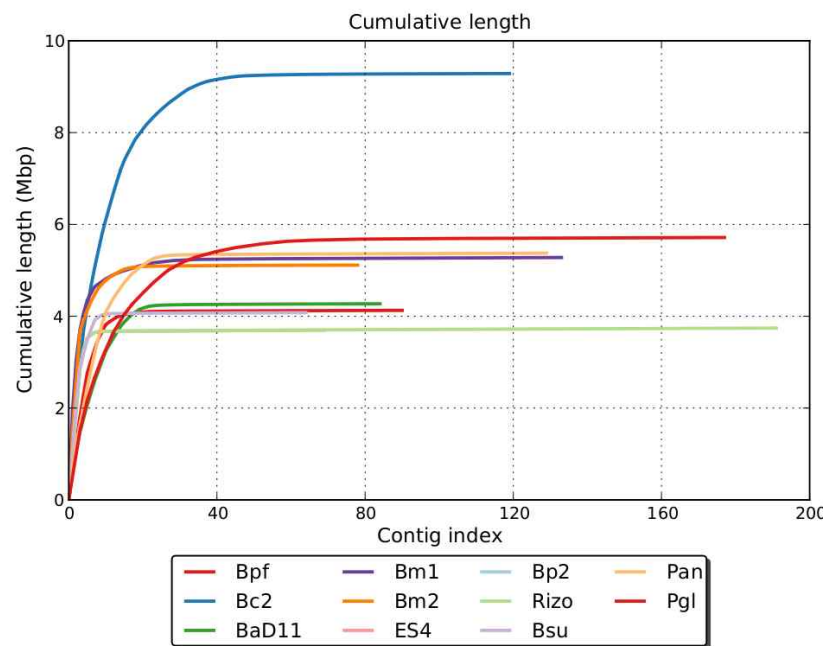


# Fig. 3

**A****B****C****D**

**Fig. 4**

**A**



**B**

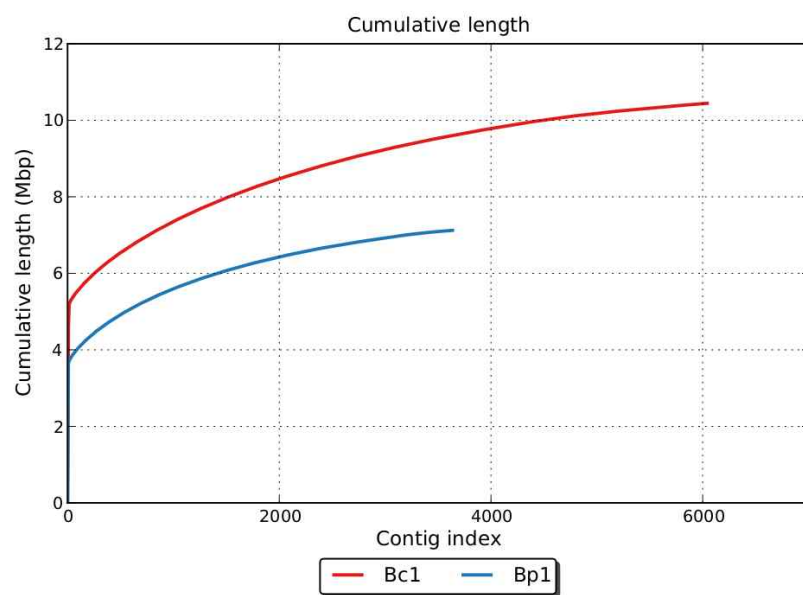


# Fig. 5

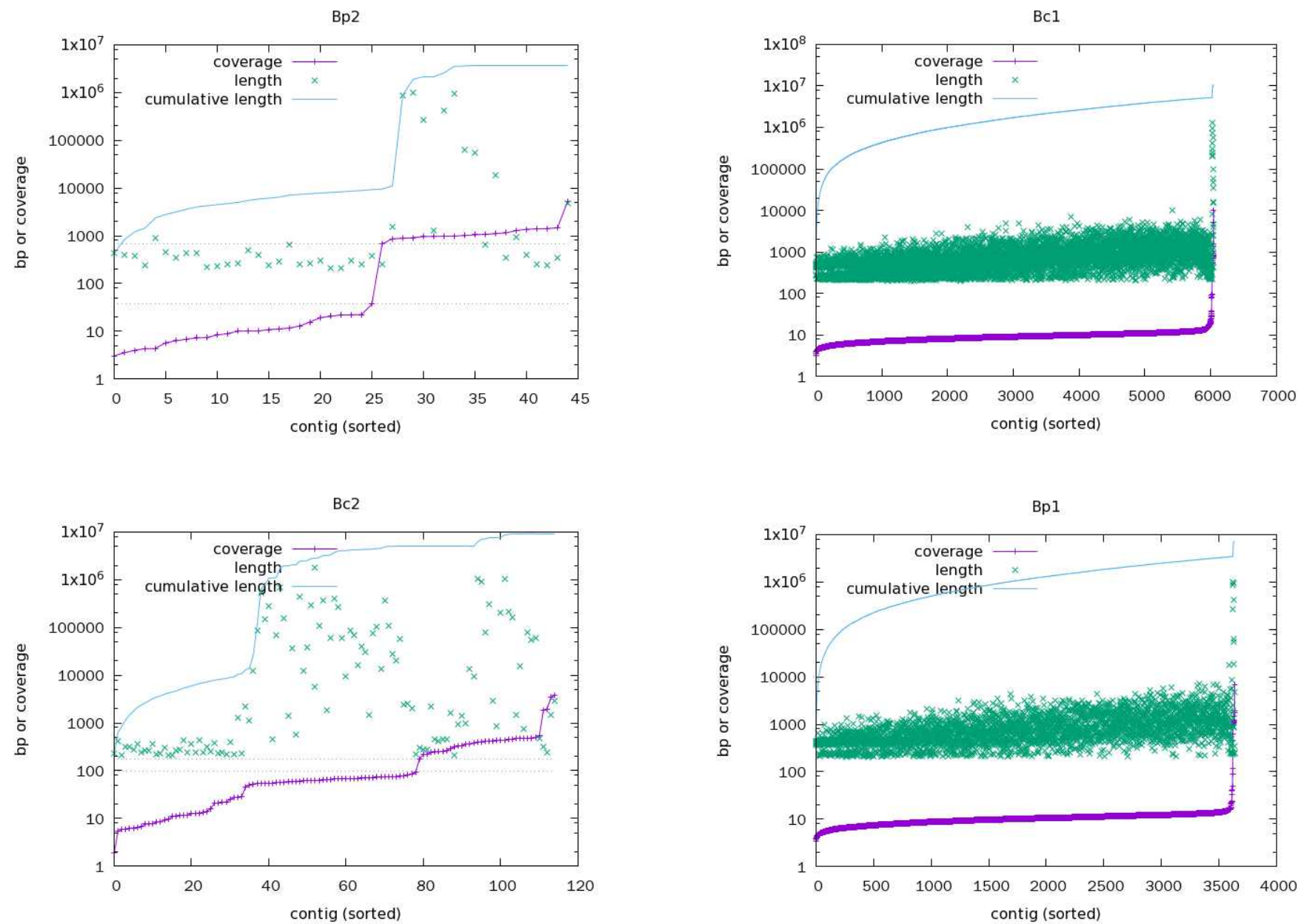
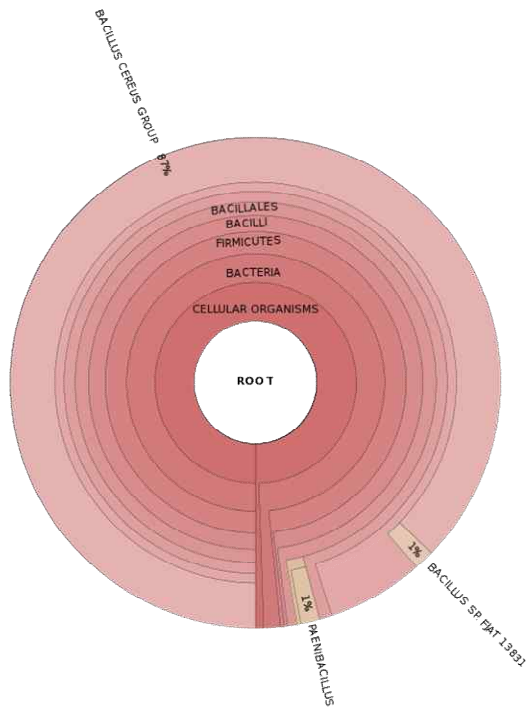
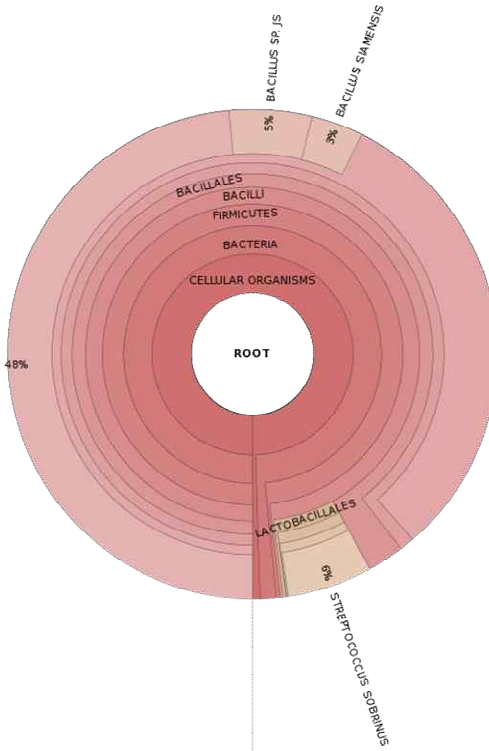


**Fig. 6**

**Bc1**



**Bc2**



**Pgl**

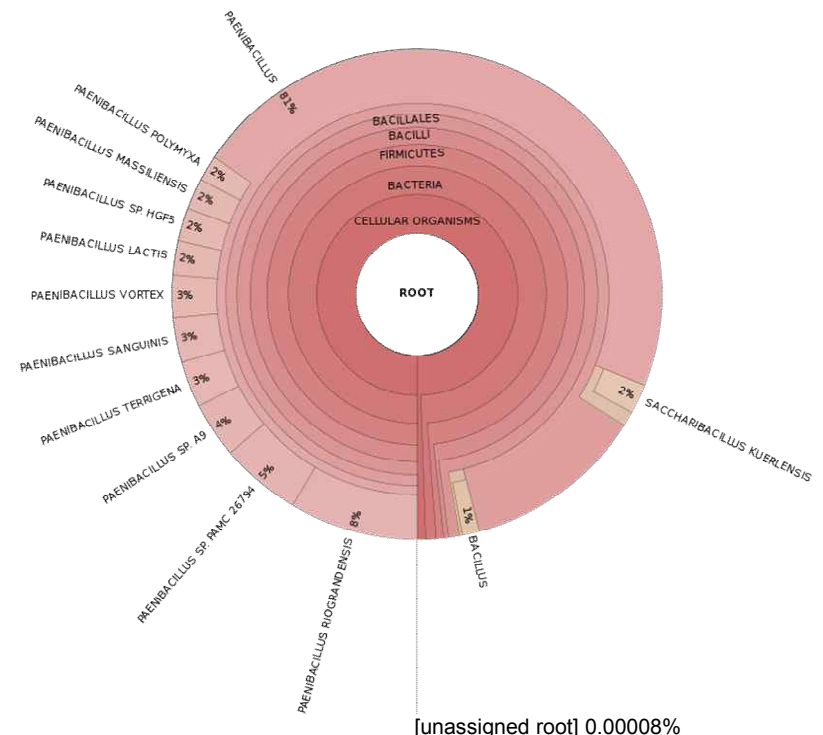


**Fig. 7**

